1.

INTRODUCTION

1.1 Introduction

In the recent years, wireless communications have been part of human life where people can communicate anywhere in the world with high speed communication. People can play the games, upload videos, surf the internet, and use social media services that have become essential part of life. To accomplish this task, Multiple Input Multiple Output (MIMO) was breakthrough in the era of mobile technology. The MIMO technologies have drawn the attention of mobile industry due to their effectiveness in increasing the speed of data transfer without requiring more spectrum efficiency [Paulraj *et al.* (2004)]. As technology became mature, the use of multi antenna systems has increased rapidly. The brief historical background and motivation for the MIMO technology are given in the following section.

1.2 Historical Background and Motivation for the MIMO Technology

In the year 1864, Maxwell proposed "Dynamical Theory of the Electromagnetic Field" [Maxwell (1864)], wherein he observed theoretically that an electromagnetic disturbance travel in free space with the velocity of light. Thereafter, Hertz discovered electromagnetic waves around year 1888 [Hertz (1888)], the result of his epoch-making experiments and related theoretical work confirmed Maxwell's predictions, and helped in the general acceptance of Maxwell's electromagnetic theory. After the confirmation of electromagnetic wave, so many experiments were performed over the electromagnetic waves to obtain different phenomenon. After successful completion of some experiments, electromagnetic waves became matured for wireless communication.

In recent years, the mobile phone technology is one of the emerging technologies in the area of wireless communication. Mobile phone technology is continuously evolving, seemingly at an accelerating rate of innovation and

adoption. The development of mobile phones started from analog system (1G: first generation) to digital system (2G: second generation), and later to third generation (3G) which can realize multimedia transmission. The first generation mobile phones were introduced in 1970s. These systems were referred as cellular. Some of the most popular standards deployed for first generation were Advanced Mobile Phone System (AMPS), Total Access Communication System (TACS), and Nordic Mobile Telephone (NMT). The analog systems were replaced by deploying the digital system (2G). In the early nineties, 2G phones were introduced by deploying Global System for Mobile Communications (GSM) technology [Radilinja's History (2009)]. An intermediary phase, 2.5G, was introduced in the late 1990s which uses the General Packet Radio Service (GPRS). The GPRS technology delivers packet-switched data capabilities to existing GSM networks. The Enhance Data Rate for GSM Evolution (EDGE) network is an example of 2.5G mobile technology. In addition to this, third generation (3G) revolution allowed mobile telephone customers to use audio, graphics, and videos applications. The 3G is a network protocol which refers to the generations of mobile phones and telecommunication equipments which are compatible with the International Mobile Telecommunications–2000 (IMT–2000) standards stated by International Telecommunication Union (ITU) [Smith and Collins (2000)]. The concept of IMT came into existence in the mid-1980s at ITU. It took more than ten years for the approval of standards for the next generation systems. These standards are branded as IMT-2000. Further, need of high speed data transfer can be fulfilled by fourth generation (4G) technology. In March 2008, International Telecommunication Union-Radio Communications Sector (ITU-R) specified a set of requirements for 4G standards, named as International Mobile Telecommunications–Advance (IMT-A) [ITU Report (2008)]. The Long Term Evolution-Advanced (LTE-A) standardized by third generation partnership project (3GPP) was approved by ITU as 4G candidate in June 2008 [3GPP Report (2013)]. The potential features of 4G technology is to provide the high performance streaming of multimedia content, high Quality of Service (QoS),

improved videos conferencing functionality, and wider bandwidth to vehicles and devices moving at high speeds within network area.

In order to further increase the data transmission rate, Multiple Input Multiple Output (MIMO) technology has became an important feature in 4G wireless communication systems. As "a key to gigabit wireless" [Paulraj *et al.* (2004)], MIMO can linearly increase channel capacity with an increase in the number of antennas without need of additional frequency spectrum and power [Foschini (1996)]. By using MIMO technology we can forget about the difficulties related to transmitting high data rates and reliable performance, and instead place the burden on the signal processing hardware in the modem. Because all the antennas transmit at the same frequencies, no extra per-user bandwidth is required from the phone tower [Vaughan and Anderson (1987)]. Spatial multiplexing is a set of clever modulation techniques that allow us to transmit independent streams from multiple antennas on the same frequencies without garbling the information. The brief discussion about the MIMO wireless communication is given in the next section.

1.3 MIMO Wireless Communication

In the conventional wireless communication system, Single Input Single Output (SISO) system is used. There is one transmitter and one receiver in SISO which is shown in Fig. 1.1(a). Both the transmitter and receiver have a common radio frequency. SISO System is used in the radio system, television system, and personal wireless technology like Bluetooth and Wireless Fidelity (Wi-Fi). In addition to the SISO system, Single Input Multiple Output (SIMO) and Multiple Input and Single Output (MISO) systems also existed. In the SIMO system, one antenna is used as transmitter and couple of antennas are used as receiver which provides diversity at receiver side and shown in Fig. 1.1(b). Whereas MISO system consists of couple of antenna at transmitter side and single antenna at receiver side which provides diversity at transmitter side and system is shown in Fig. 1.1(c). Further, MIMO technology has attracted much attention in wireless communications, because it offers significant increases in data throughput and

link range without additional bandwidth or increased transmit power. It achieves the goal by spreading the same total transmit power over the antennas to achieve an array gain that improves the spectral efficiency (more bits per second per hertz of bandwidth) and/or to achieve a diversity gain that improves the link reliability (reduced fading). Because of these properties, MIMO is an important part of modern wireless communication standards such as IEEE 802.11n (Wi-Fi), 4G, 3GPP Long Term Evolution, WiMAX and HSPA+.

The modelled system of MIMO is shown in Fig. 1.1 (d). The channel includes scattering objects between the transmitter and receiver. The input signal vector $\boldsymbol{X}$ and the output signal vector $\boldsymbol{Y}$ are related through the channel matrix $\boldsymbol{H}$ after adding the Additive White Gaussian Noise (AWGN) vector $\boldsymbol{n}$.

$$\boldsymbol{Y=HX+n} \tag{1.1}$$

Without the Channel State Information (CSI) at the transmitter, the power is equally allocated to the individual transmitter. The total transmitted power p_t is constrained by the covariance matrix $\boldsymbol{R}_{xx} = E\{\boldsymbol{x}\boldsymbol{x}^{\boldsymbol{H}}\}$, satisfying $\mathrm{Tr}(\boldsymbol{R}_{xx}) = p_t$.

The elements of channel matrix $\boldsymbol{H}$ are related to the transmission coefficient between transmit and receive antennas of the system [Winter (1987)] and is computed as;

$$H = \begin{bmatrix} h_{11} & \cdots & h_{1M} \\ \vdots & \ddots & \vdots \\ h_{N1} & \cdots & h_{NM} \end{bmatrix} \tag{1.2}$$

$$h_{rt} = S_{ij},\ r = 1,\ldots, N \text{ and } t = 1,\ldots, M$$

where, $S_{ij},\ j = 1, \ldots, M; i = M + 1 \ldots, M + N$ is the complex transmission coefficient between the j^{th} transmit antenna and the i^{th} receive antenna. Each element of $\boldsymbol{H}$ can be decomposed into two main components;

$$S_{ij} = S_{ij}^{d} + S_{ij}^{m} \tag{1.3}$$

where, S_{ij}^{d} is the direct component and S_{ij}^{m} is the super position of all multipath components. The capacity of $\boldsymbol{M} \times \boldsymbol{N}$ MIMO channel is given by [Foschini and Gans (1998)],

$$C = log_2 \left\{ \left| \boldsymbol{I} + \frac{SNR}{M} \boldsymbol{H}\boldsymbol{H}^{\dagger} \right| \right\} \text{ bits/s/Hz} \tag{1.4}$$

where, $\boldsymbol{I}$ is an $N \times N$ identity matrix and † is the conjugate transpose of the corresponding matrix and SNR= p_t/σ^2 where σ^2 is the noise power.

This thesis is focused on the implementation of Multi Antenna System (MAS) inside the handheld devices like smart mobile phones, laptop, USB dongle etc. However, the trend in mobile devices technology in the recent years is to dramatically decrease the size and the weight of the device, forcing designers to come up with highly compact designs. It has been proved from so far research that there are some fundamental limitations and trade-offs between the physical size of an antenna and its gain, efficiency, and bandwidth. So, one has to make some kind of compromise among volume, impedance bandwidth and radiation characteristics of an antenna.

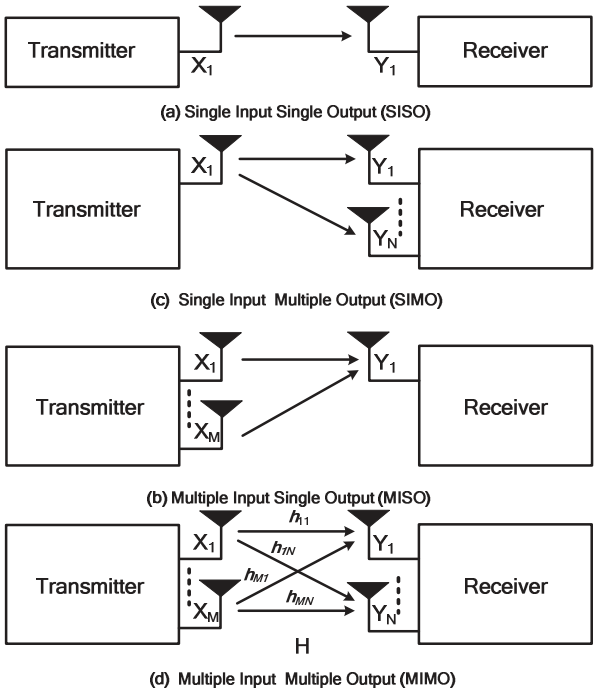

Figure 1.1: (a) SISO system, (b) SIMO system, (c) MISO system, and (d) MIMO system.

1.4 Various Promising Internal Antennas

As per the wave propagation theory, the radiation capability of an antenna depends on its wavelength for the designed frequency. Initially, antenna was placed external to the mobile phone and such types of antenna are called as monopole antenna (a Whip antenna). A monopole antenna had excellent performance, especially when the main PCB of the handset was also a quarter-wavelength, forming a half-wavelength unbalanced dipole. These phones were quite large, with a total size of ~160-170 mm, corresponding to a half-wavelength at 800-900 MHz [Sandell (1997)]. However, the conventional microstrip patch antennas are also based on half-wavelength of operation [Balanis (2005), Pozar (1995)] but are not a good candidate for the portable devices as their designs do not meet the strict small space requirement of these devices. Therefore, more unusual approaches must be examined for compact antenna design.

As the time passes, technology of mobile phones has dramatically changed and antenna technology is also changed simultaneously. The externally placed antennas in mobile phone become internal. Some of the essential factors to be considered in antenna design for modern day portable devices are as follow:

- Small size and light weight
- Robustness
- Flexibility
- Multiband
- Built-in
- Easy to integrate

In view of the above, two types of internal antennas for mobile phones are considered in this thesis and are discussed below:

1.4.1 Planar Inverted-F Antenna (PIFA)

In the past decade, the Planar Inverted-F Antenna (PIFA) has been used extensively in wireless communication devices operating in the frequency bands for Wireless Local Area Network (WLAN) and Worldwide Interoperability for

Microwave Access (WiMAX) (2.4, 3.4, 3.7 and 5 GHz) and some other wireless applications [Soras *et al.* (2002), Geyi *et al.* (2008)]. The PIFA is well-suited for these applications because its physical size is reasonable with the dimensions of the intended wireless devices.

A PIFA is generally considered to be a microstrip antenna on a finite ground plane with a ground connection. The PIFA can be realized as combination of the Inverted-F Antenna (IFA) and the Short-Circuited Microstrip Antennas (SC-MSA). Both IFA and SC-MSA have narrow band characteristics, itself. In the PIFA, wire radiator element of the IFA is replaced by a plate to expand the bandwidth. The schematic and front view of PIFA is shown in Fig. 1.2. It consists of a main radiating arm named as patch that is parallel to the ground plane. This patch is connected to the ground plane via shorting plate/pin at its one end. The feed is placed between the open and shorted end of the patch and, the distance between the shorted end and feed point control the input impedance of the antenna structure.

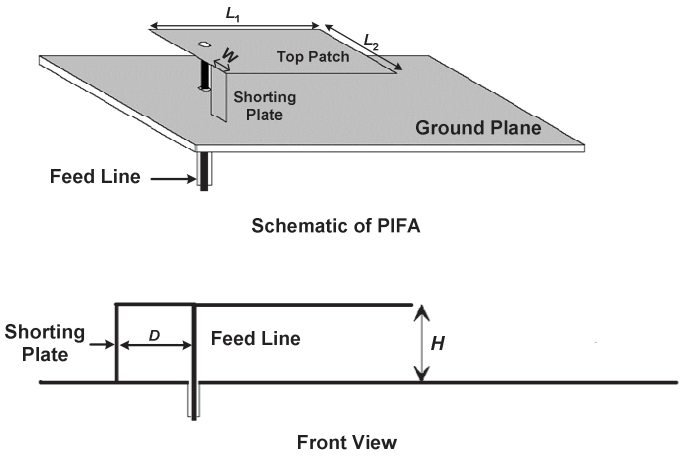

Figure 1.2: Schematic and front view of the PIFA.

1.4.1.1 Design Methodology of PIFA

The length and width of top patch of the PIFA are L_1 and L_2, respectively and is shown in Fig. 1.2. The one terminal is short circuited though shorting plate of width W and feeding point is located near to the shorted edge of the PIFA. The

impedance of the PIFA can be controlled by the distance *D* of the feed to the shorting plate. The distance *D* between the shorting plate and the feed point can be used to control the reactive impedance of the antenna. The value of the reactive impedance is inversely proportional to the value of *D* [Soras *et al.* (2002)]. By varying the distance *D*, the reactive impedance may be cancelled, resulting in real input impedance. The PIFA can have its impedance tuned with this parameter also.

The quarter wave resonating behaviour of PIFA is determined by its length (L_1) and width (L_2) and is given as [Garg *et al.* (2001)]:

$$L_1 + L_1 = \frac{\lambda}{4}$$

Therefore,

$$f = \frac{c}{4(L_1+L_2)} \tag{1.5}$$

where, c is speed of light in free space and λ is wavelength at resonating frequency.

The resonance frequency of PIFA also depends on width (W) of shorting plate. Few cases are considered to determine the resonance frequency of PIFA.

Case I: When $W = L_2$, this is the case when the width (W) of the shorting plate is equal to the width of the top patch i.e. L_2. This corresponds to the case of the short circuit of patch, which is a quarter-wavelength antenna. The effective length of the patch is $L_1 + H$ where, H is the height of the shorting plate. The resonance condition then is expressed as:

$$L_1 + H = \frac{\lambda}{4}$$

Therefore,

$$f = \frac{c}{4(L_1+H)} \tag{1.6}$$

This is the case when PIFA has maximum radiation efficiency.

Case II: When $W = 0$, this is case when short circuit plate is considered as thin short-circuit pin. The effective length of the patch is $L_1 + L_2 + H$. For this case, the resonance condition is expressed as:

$$L_1 + L_2 + H = \frac{\lambda}{4}$$

Therefore,

$$f = \frac{c}{4(L_1+L_2+H)} \tag{1.7}$$

This case acts as microstrip antenna because shorting plate is considered of negligible thickness. So the electrical length of current over patch is considered as from clockwise direction (from feed point to the open edge of patch) and counter clockwise direction (from open edge of PIFA to the feed point). The clockwise and counter-clockwise paths always add up to $2*(L_1+L_2)$, so on average, resonance will occur when the path length (L_1+L_2) for a single path is quarter-wavelength.

Case III: When $0 < W < L_1$, the resonant frequency f is a linear combination of the resonant frequencies associated with the limiting cases and is given as:

$$L_1 + L_2 + H - W = \frac{\lambda}{4}$$

Therefore,

$$f = \frac{c}{4(L_1+L_2+H-W)} \tag{1.8}$$

Case IV: The resonant frequency also depends on the diameter of the through hole in substrate in addition to the length and width of the patch. If diameter of the through hole substrate is *d*, the resonant frequency is determined as [Ogawa and Uwano (1994)].

$$f = \frac{c}{4(L_1+L_2+\pi d)} \tag{1.9}$$

From the study of different cases it can be concluded that the resonance frequency can be tuned by using width of short circuited plate, by adjusting the height of main radiating elements from ground plane, and diameter (*d*) of the probe through which feeding in given to patch. The position of feed point may

also be helpful in resonance frequency tuning. Further, reduction in resonance frequency can be achieved by embedding open slots. The open slot on the radiating patch leads to the flow of current at the edge of the shaped slot, therefore a capacitive loaded slot reduces the frequency and thus the antenna dimensions drastically reduces. The same principle of making slots in the planar element can be applied for dual-frequency operation as well.

1.4.1.2 Radiation Mechanism of PIFA

The radiation mechanism of the PIFA can be understood with the help of half wave length microstrip patch antenna. For a half wavelength patch antenna, the electrical field distribution under the patch is given by $E_0 \cos(\pi x/L)$, with a maximum electric field at one of the radiating edge, zero in the middle (i.e. at $x = L/2$), becoming maximum again at the other radiating edge with 180^0 phase reversal as shown in Fig. 1.3(a).

- Since the electric field is zero at the half of the patch say $x=L/2$, an electric wall can be placed there without disturbing the field distribution under the patch. The electrical wall directly connected with ground plane (now patch is short circuited at half of the portion). One half of this patch can now be discarded. The patch will still be resonant at the design frequency of a half wave rectangular patch. This type of patch geometry is called a quarter-wave patch [Fig. 1.3 (b)] as the separation between the radiating edge and the electric wall is about $\lambda_g/4$. A major difference between the half-wave patch and the quarter-wave patch is that the quarter-wave patch has one radiating edge compared to two for the half-wave patch [Garg *et al.* (2001)]. This physical difference is responsible for all the differences in antenna characteristics, which are given below.

- The *E*-plane pattern of the quarter-wave patch becomes broader because the array effect of the two radiating edges for a half-wave patch is absent here. Also, the half-length nature of the patch gives rise to a cross-polarized E_θ component in the *H*-plane.

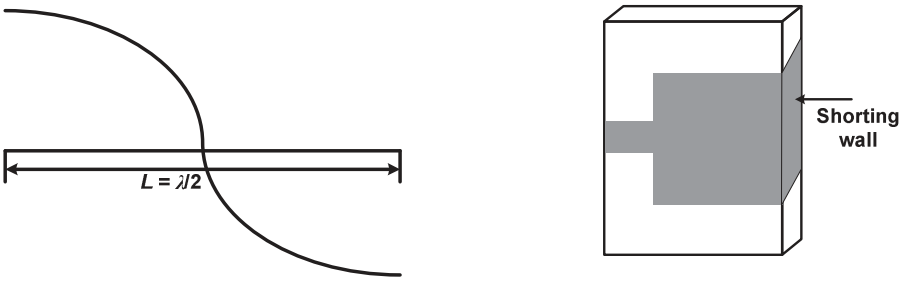

Figure 1.3: (a) Electric field distribution along patch resonant length and (b) Quarter wave patch, shorted at one end.

- The radiation conductance G_r of a quarter-wave patch is due to radiation from a single edge. Its value is lower by a factor of about 2 compared to that of a half-wavelength patch. Therefore, the radiation resistance at resonance will be about two times.
- The stored energy in a quarter-wave patch is exactly one-half that of the half-wave patch because of identical field distribution over half the area.
- Q factor calculations shows that bandwidth of the quarter-wave patch is about the same as that of half-wave patch.

1.4.1.3 Advantages of PIFA

The PIFA having several advantages over simple microstrip antenna which are listed below:

- PIFA can be fitted into the housing of the mobile phones easily as compared to the whip/rod/helix antennas.
- PIFA having reduced backward wave radiation towards the user head, minimizing the absorption of electromagnetic energy inside the human tissues and enhance the antenna performances.
- PIFA exhibits moderate to high gain in both vertical and horizontal states of polarization. This feature is very useful in certain wireless

communication where the antenna orientation is not fixed and reflections are present from different corners of the environment.

From the above discussions about PIFA, it can be concluded that the PIFA may be a preferable candidate for the mobile phone application because it has several properties which are compatible to the mobile phones. The compatibility of size, low Specific Absorption Rate (SAR), and radiation performances makes it suitable for modern mobile phone applications.

In addition to the PIFA there are some other antennas have been evaluated for portable devices which can also be suitable for mobile phone applications. In this context planar monopole antenna is chosen for study in this thesis due to its highest suitability among other available antennas.

1.4.2 Planar Monopole Antenna (PMA)

Planar monopole antenna is also a promising internal antenna which can be easily fitted inside the mobile phone. The branched monopole antenna mentioned here can be built with a very low profile form. Then it can easily be accommodated within the housing of a mobile handset.

Initially, monopole antennas are typically classified as external antennas with the quarter wavelength wire antenna (whip) or the helix antenna. But monopole antenna can be an internal antenna if it is an antenna without a ground plane directly underneath it. They are referred as planar monopole antenna or PMA. The PMA usually has a long branch to tune the lower frequency band and a short branch to tune the higher frequency band. It can also combine a non-uniform meander and a branch to enhance the bandwidth [Andersson (2002)]. When the chassis of the handset is less than a quarter wavelength, the bandwidth will be reduced. The monopole can be capacitively coupled or matched to the terminal housing to excite the chassis mode to gain some extra bandwidth when the chassis length is larger than a quarter wavelength, by combining the antenna modes and chassis modes of the multi resonant structure. When the height of the low profile monopole is too low, the antenna becomes capacitive, then an extra ground pin is

needed to form a matching loop, and the antenna becomes a branch IFA or non grounding PIFA. Some of the well fitted PMA inside the mobile phones are shown in Fig. 1.4.

1.4.2.1 Design Methodology of PMA

A monopole antenna is one half of a dipole antenna which is mounted above sort of ground plane. The monopole antenna is derived by dipole antenna by applying the image theory. A monopole antenna can be visualized as being formed by replacing the bottom half of a vertical dipole antenna with a conducting plane (ground plane) at right-angles to the remaining half. If the ground plane is large enough, the radio waves from the remaining upper half of the dipole reflected from the ground plane will seem to come from an image antenna [Stutzman (1981)]. The quarter wave monopole antenna and equivalent half wave dipole antenna are shown in Fig. 1.5.

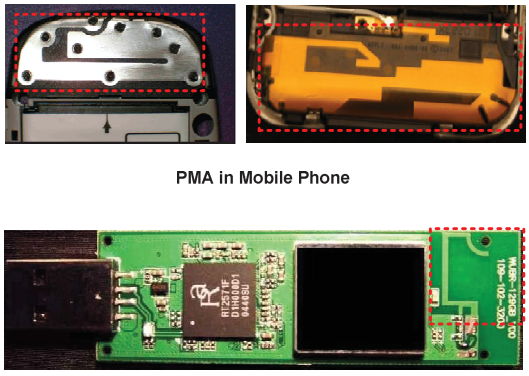

Figure 1.4: Planar monopole antenna inside portable devices.

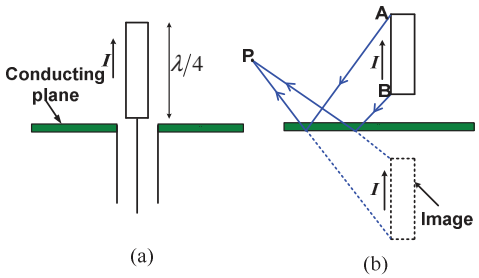

Figure 1.5: (a) Quarter wave monopole antenna and (b) Equivalent half wave dipole antenna.

Since the current and charges on the monopole are the same as on upper half of its dipole counterpart, but the terminal voltage is only half that of the dipole. The voltage is half because the gap width of the input terminal is half that of the dipole and same electric field over half the distance give half the voltage. The input impedance of the monopole is therefore half that of its dipole counterpart, or

$$Z_{in} = \frac{V_{in,mono}}{I_{in,mono}} = \frac{\frac{1}{2}V_{in,dipole}}{I_{in,dipole}} = \frac{1}{2}Z_{in,dipole} \tag{1.10}$$

This is easily demonstrated for radiation resistance. Since the field only extended over a hemisphere the power radiated is only half of a dipole with the same current. Therefore, radiation resistance of the monopole is given as [20]:

$$R_{r,mono} = \frac{P_{rad,mono}}{\frac{1}{2}|I_{in,mono}|^2} = \frac{\frac{1}{2}P_{rad,dipole}}{\frac{1}{2}|I_{in,dipole}|^2} = \frac{1}{2}R_{r,dipole} \tag{1.11}$$

1.4.2.2 Radiation Mechanism of PMA

Single-ended sources may be used without baluns when monopole antennas are used. When placed over a conducting ground plane, a quarter-wave monopole antenna excited by a source at its base as shown in Fig. 1.5 (a) exhibits the same radiation pattern in the region above the ground as a half-wave dipole in free space. This is because, from image theory, the conducting plane can be replaced with the image of a λ/4 monopole, image of upper half of dipole is shown in Fig. 1.5 (b). However, the monopole antenna can only radiate above the ground plane. Therefore, the radiated power is limited to $0 \leq \theta \leq \pi/2$. Hence the λ/4 monopole radiates only half as much power as the dipole [Stutzman (1981)].

However, the radiation patterns of a monopole above a perfect ground plane is the same as that of a dipole similarly positioned in free space. Since the fields above the image plane are the same. Therefore, a monopole above perfect ground plane radiates one half the total power of a similar dipole in free space because the power is distributed in same fashion but only over half space. Since, the impact of

ground plane shape and size is important factor during the design of PMA so the study of ground plane effect is important.

1.4.2.3 Advantages of PMA [Fujimoto (2008)]

The advantages of PMA are listed below:

- PMA have more degree of freedom to design an antenna for portable terminals
- It has thin profile structure
- Performance is similar to the externally placed monopole antenna (Whip)
- The multi branches PMA have the multi resonance nature
- It has wider bandwidth characteristics

From the above discussions, it can be concluded that the PMA may also be one of the promising internal antenna candidate for mobile phone application.

In the last decade MIMO antenna has enormous attention of the researchers, and its development is more rapid than ever before. MIMO antenna systems have the potential to become one of the most important components in the next generation of high performance mobile communication systems. The MIMO is a promising antenna structure for mobile phones, laptop, and Universal Serial Bus (USB) dongle to achieve high data transfer speed and better quality of communication. The current market demand is towards antenna miniaturization with enhanced number of applications. In addition to antenna design, performance of antenna within actual scenario is also an important factor.

In a compact MIMO/Diversity antenna terminal, the space for the multi antenna system is quite limited, which would results in high mutual coupling and degrade the performances of multi antenna system. Currently, PIFA and PMA have been widely designed for portable devices due to their compact and low profile structure as well as low manufacturing cost. When number of PIFA and PMA share common ground plane, performances of individual antenna may

degrade. In view of this, it is important to reduce the mutual coupling between antenna elements for satisfactory operation of each antenna elements of MIMO configuration. Some of the researchers have applied various isolation techniques to enhance the isolation. The next section demonstrates the isolation enhancement techniques between MIMO antenna elements.

1.5 Isolation Enhancement Techniques

A common problem with MIMO antenna system is lack of electromagnetic isolation between closely spaced antennas within small portable devices. There are number of isolation enhancement techniques are available in the literature which are discussed below:

1.5.1 Defected Ground Structure (DGS)

A DGS may come in a variety of shapes and sizes depending upon their mode of application, as well as the frequency of operation. There are different shapes like rectangular dumbbell [Kim *et al.* (2000)], circular dumbbell [Rahman *et al.* (2004)], spiral [Kim *et al.* (2002)], 'U' and 'V' [Woo *et al.* (2006)], 'H' [Mandal and Sanyal (2006)], cross [Chen *et al.* (2006)], concentric rings [Guha *et al.* (2006)], etc., as illustrated in Fig. 1.6. Some complex shapes have also been studied which include meander lines [Balalem *et al.* (2007)], split ring resonators [Hou (2008), Burokur *et al.* (2005)], and fractals [Liu *et al.* (2003)]. Conventionally, in planar microstrip circuits, a DGS is located beneath a microstrip line and it perturbs the electromagnetic fields around the defect. Trapped electric fields give rise to the capacitive effect (C), while the surface currents around the defect cause an inductive effect (L).

In multi antenna system, DGS plays significant role in isolation enhancement by suppressing surface current on ground plane. The DGS perturbs the electromagnetic field between MIMO antenna elements and hence achieved improved isolation between multi antenna ports.

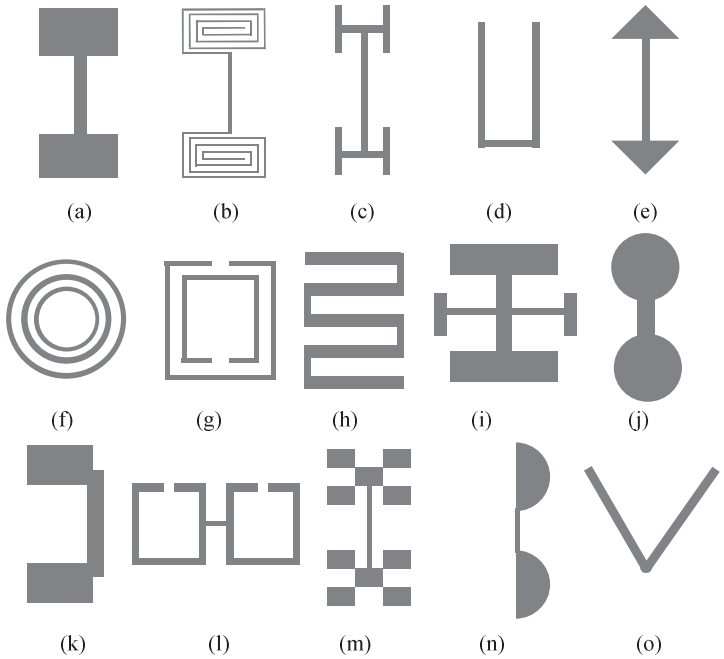

Figure 1.6: Different DGS geometries: (a) Dumbbell-shaped, (b) Spiral-shaped, (c) H-shaped, (d) U-shaped, (e) Arrow head Dumbbell, (f) Concentric ring shaped, (g) Split ring resonators, (h) Meander line, (i) Cross-shaped, (j) Circular head dumbbell, (k) Square heads connected with U-slots, (l) Open loop dumbbell, (m) Fractal, (n) Half-circle, and (o) V-shaped.

1.5.2 Neutralization Line

The existing mutual coupling is due to capacitive coupling between the main plates of the PIFAs, magnetic coupling between the facing shorting strips and a strong coupling via the electrical currents which are flowing on the PCB from one port to the other. Neutralization technique is one of the promising solutions to enhance isolation between multi antenna elements as shown in Fig. 1.7. It is based on field cancelling concept between two antennas. The principle of the neutralisation technique is the compensation for the existing electromagnetic coupling between the two antennas of the structure, through a direct connection via a suspended link.

Some of the neutralization techniques have been suggested in [Diallo *et al.* (2006), Su *et al.* (2012)] to improve isolation by utilizing a field cancelling concept. In [Diallo *et al.* (2006)], antennas are designed for the DCS and UMTS

bands and studied the mutual coupling between them by considering the feeding strip facing and shorting strip facing cases. They used a single suspended line of different lengths for cancelling the fields and about -20 dB isolation was achieved. Some of the neutralization line techniques have been applied to enhance the isolation between ports as shown in Fig. 1.7.

1.5.3 Electromagnetic Bandgap (EBG) Structure

EBGs are a class of metamaterials whose purpose is to offer high impedance to the electromagnetic propagation along the device surface within the frequency band of operation known as a "band gap" (hence the name "electromagnetic band gap" material).

EBG structures are one of the possible solutions to improve the isolation between two antenna elements. EBG is a new type of engineered surface which block current flowing at microwave frequencies. EBG material is a periodic surface specifically designed to have certain electromagnetic properties at specific frequencies.

An EBG is employed between the multi antenna systems to improve the electromagnetic isolation between them. The different geometry of EBG unit cells creates extra inductances and capacitances for electromagnetic waves. When the unit cell is properly tuned, the aggregate surface will block incoming signals just as a band stop filter. This improved isolation allows operating multi elements of MIMO configuration individually. Some of the EBG structures are proposed by researchers for isolation improvement [Hsu *et al.* (2011), Lee *et al.* (2012a)] as shown in Fig. 1.8.

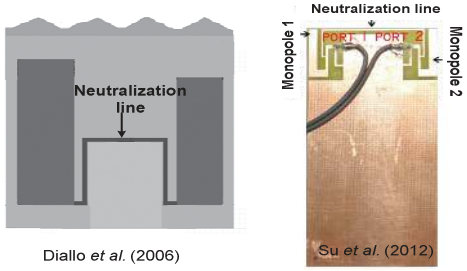

Figure 1.7: Neutralization line between multi antenna systems.

1.5.4 Dielectric Wall Loading

Dielectric Materials are electrical insulators or materials in which electric field can be sustained with a minimal dissipation of power. They are characterized by the dielectric permittivity (ε_r), that is a measure of how electric field affects, and is affected by a dielectric medium [Abelairas *et al.* (2009)]. It is determined by the ability of a material to polarize in response to the field. The placement of dielectric wall between the MIMO antennas not only improves isolation but also change its resonance frequency. For this reason, once the dielectric wall is placed on the ground plane the antenna has to be retuned, because its resonance frequency may be shifted to lower frequency side. The change experienced by the resonance frequency depends on the features of the dielectric wall. These are the permittivity, the size of the wall, and its position on the ground plane. Some of the researchers have proposed dielectric wall between antenna elements to improve the isolation which is shown in Fig. 1.9.

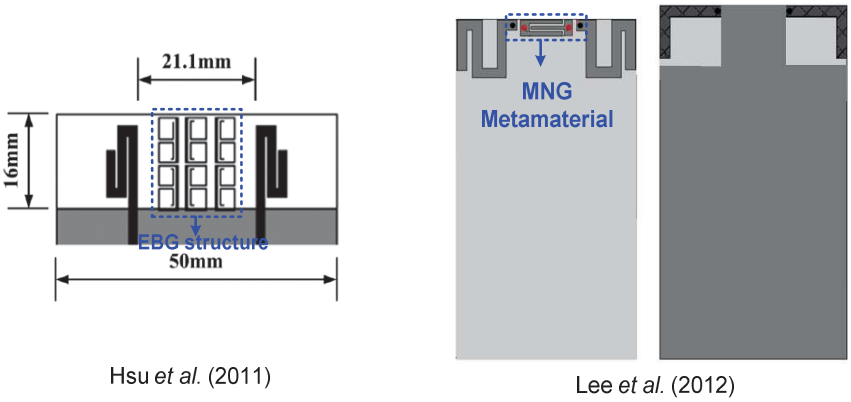

Figure 1.8: EBG structure between MIMO antenna elements.

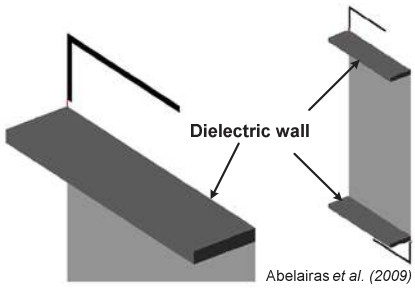

Figure 1.9: Loading of dielectric wall between MIMO antennas for isolation.

1.5.5 External Feed Network

External feed network is one of the possible solutions to improve the isolation between antenna elements. Chen *et al.* proposed four port decoupling network. In decoupling network, two output ports are directly connected to the radiating antenna elements to reduce the mutual coupling and two ports are connected with matching network for improving the impedance matching [Chen *et al.* (2008)]. The decoupling network consists of two transmission lines in order to transform the complex trans-admittance to a pure imaginary one. A shunt reactive component is then attached in between the transmission lines ends to cancel the resultant imaginary trans-admittance. Finally, a simple lumped-element circuit is added to each port for input impedance matching. The decoupling network is shown in Fig. 1.10(a).

An LC-based branch-line hybrid coupler was integrated with the Long Term Evolution (LTE) antenna array [Bhatti *et al.* (2009a)] as shown in Fig. 1.10(b). The branch-line hybrid coupler is designed at 710 MHz using the passive inductors and capacitors. Each quarter wavelength transmission line section of the branch line coupler has been integrated with the antenna array to decouple the antenna ports. The two monopole antennas have been attached to the hybrid coupler ports 3 and 4, respectively. Ports 1 and 2 of the hybrid coupler are decoupled, which are connected to the input ports.

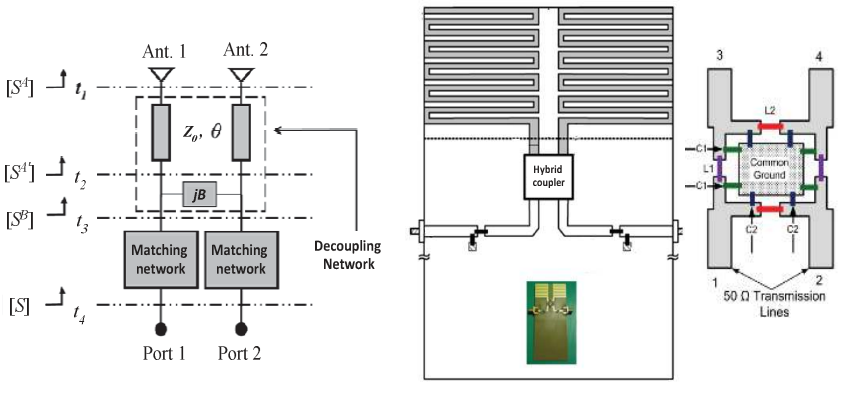

(a) Chen *et al.* (2008)

(b) Bhatti *et al.* (2009a)

Figure 1.10: External feed network for isolation improvement and (a) Decoupling network, (b) Branch-line decoupling feed network.

1.5.6 Orientation of the Multi Antenna Systems

The isolation between multi element antennas of MIMO configuration also depends on the orientation of elements over the shared ground plane of the PCB. In general, isolation can be improved by increasing the spacing between antenna elements. Good isolation can be achieved by keeping the separation between antenna elements more than half wavelength. However, this spacing is usually limited (especially at low frequencies), particularly for a mobile terminal which has very restricted size for the antennas. So, in order to solve the problem of isolation within confined space of mobile phones, mutual orientation of multi antenna elements over PCB is important. When multiple antennas are collocated on a single device, some factors such as the antenna positions relative to each other and to the ground plane influence the radiation. In addition, applications such as mobile phones, the ground plane or device chassis is considered as part of the antenna and therefore contributes to the radiation. Therefore, it is important to find the appropriate configuration of antennas which can satisfy all the system requirements. Jakobsen and Thaysen investigated fifteen symmetrical and asymmetrical coupling scenario using two identical PIFAs on an infinite ground plane [Jakobsen and Thaysen (2007)].

However, the orientation of antennas perpendicular to each other over mobile circuit board is one of the better solutions for isolation enhancement within the confined space of mobile phone. The other way to decrease the correlation is using multiple antennas with different radiation patterns. It is better to have the patterns complementary to each other in space for receiving multipath signals from different directions. This phenomenon can be achieved by positioning the antenna with its mirror image over mobile circuit board.

From the above discussion of isolation enhancement techniques, it is found that neutralization line occupies larger area over the mobile circuit board while EBG structures require an intricate fabrication process. The loading of dielectric wall between MIMO antenna elements makes whole system much heavy and external feeding networks are complicated in terms of fabrication and placement within the

confined space of mobile circuit board. Further, orientation of antennas over mobile circuit board is not possible solution because within mobile circuit board, constraint of limited space does not allow degree of freedom for antenna designer to design such orientation.

In view of the above, in this thesis folded shorting strips and protruded ground plane are used to enhance the isolation between MIMO antenna elements. The folded shorting strips are proposed and investigated the effect on isolation characteristics. The folded shorting strip is placed at the end of the PCB so that other mobile circuitries can easily be mounted. Further, protruded ground plane is used between multi antenna systems to improve isolation.

Based on the above discussion about PIFA and PMA for MIMO applications and isolation enhancement techniques for MIMO elements, literature reviews are given below.

1.6 Literature Review

In this section, literature survey is carried on the available literature related to multiband/wideband MIMO antennas for mobile phone and USB dongle applications. When MIMO antenna elements are placed within small devices, isolation becomes crucial parameters. So literature review on isolation between MIMO antenna elements is also done in this thesis. However, the implementation of MIMO antenna system in portable devices starts since 1986.

The built-in diversity antenna for 800 MHz band portable radio unit was first time implemented by Taga and Tsunekawa in 1986 [Taga and Tsunekawa (1986)]. In 1994, Ogawa and Uwano [Ogawa and Uwano (1994)] investigated diversity antenna which compromising short whip top loaded with a small cylinder and a new built-in antenna for very small portable telephones in the 800 MHz band. Ogawa *et al.* analysed the performance of a handsets diversity antenna in the presence of head, hand, and shoulder at 900 MHz [Ogawa *et al.* (1999)]. Further, in 2000 Ogawa and groups investigated the Mean Effective Gain (MEG) characteristics in the presence of mobile environment [Ogawa *et al.* (2000)].

Again in 2001, Ogawa and groups analysed the effective gain characteristics and correlation characteristics in the Part I and Part II, respectively [Ogawa *et al.* (2001a), Ogawa *et al.* (2001b)]. Also, the diversity characteristics investigated in the presence of user proximity (head, hand, and shoulder).

After the investigation of some diversity antenna systems, MIMO technology became mature and ready to implement inside the mobile devices. In order to do this, Wu *et al.* in 2002 presented a printed diversity monopole antenna for WLAN operation in the 2.4 GHz band. The antenna comprised two orthogonal linear monopoles placed symmetrically with respect to a T-shaped ground plane between them [Wu *et al.* (2002)]. Same authors' group investigated a antenna which comprised two substantially orthogonal printed monopoles with a straight strip of longer length for the lower band operation (2.4 GHz band) and protruded strip of shorted length for the upper band operation (5.2 GHz band) in 2003 [Wu *et al.* (2003)]. Karaboikis *et al.* demonstrated a dual-printed inverted-F antenna diversity systems for terminal devices operating at 5.2 GHz under both switched and combining schemes [Karabooikis *et al.* (2004)]. Soon after, Chi *et al.* presented dual band printed diversity antenna for 2.4/5.2 GHz WLAN operation which consisted of two orthogonal C-shaped monopoles and placed symmetrically with respect to a protruding T-shaped ground plane [Chi *et al.* (2005)]. Thereafter, Yeap *et al.* proposed a low profile diversity antenna for MIMO applications in 2006. The design of the antenna was based on a double folded dipole antenna filled with a slab of ceramic of $\varepsilon_r = 6$ [Yeap *et al.* (2006)]. Further, Wong *et al.* designed a printed collinear two antenna elements suitable for application in a WLAN access point in MIMO system [Wong *et al.* (2006a)]. Later on, Wong *et al.* analyzed three electromagnetic compatible (EMC) chip antennas for Personal Digital Assistant (PDA) phone application [Wong *et al.* (2006b)].

In 2007, Chung and Yoon presented a MIMO antenna which comprised two folded monopoles and was designed to operate in WiBro (Wireless Broadband Internet; the Korean version of mobile WiMax) service band, 2.30–2.39 GHz. Further, to decrease mutual coupling between the antennas, ground wall and

connecting lines are added [Chung and Yoon (2007)]. Later, Chiu *et al.* designed a slitted ground plane between antenna elements to suppress the mutual coupling between closely packed antenna elements [Chiu *et al.* (2007a)]. In the same year, Shin and Park described a printed diversity planar monopole antenna integrated on a PCMCIA network card which minimized the mutual coupling for WLAN application at 5 GHz band [Shin and Park (2007)]. Further, Chen *et al.* investigated a high performance monopole antenna fabricated using folded wire line and a metal patch as radiator [Chen *et al.* (2007)]. Soon after, Ding *et al.* described four printed monopole antennas that occupy relatively small area at the four corners of a printed circuit board (PCB) and each antenna element lid of a folder-type mobile phone [Ding *et al.* (2007)]. Further, Chiu *et al.* demonstrated three-port orthogonally polarized antennas using dipole antennas and half-slot antennas. Each of the antennas constituted by three mutually perpendicular radiating elements to achieve good isolation and low antenna signal correlation between ports [Chiu *et al.* (2007b)].

In 2008, Hui and Tiong suggested a dual-monopole array backed by a plane reflector and rigorously analysed to provide information on the installations and applications of monopole arrays mounted on a wall or ceiling for antenna diversity/MIMO operations [Hui and Tiong (2008)]. Further, Chiu *et al.* investigated a 24-port and 36-port antennas based on a cube structure. The antennas was formed by densely packed individual antennas on a cube. The 24-port antenna cube has a volume of $0.72\lambda_0^3$ while the 36-port antenna had a volume of $1.13\lambda_0^3$ [Chiu *et al.* (2008)]. There after, Diallo *et al.* described two PIFAs, closely positioned at the top edge of a small ground plane whose size was representative of the printed circuit board of a mobile phone. To enhance the isolation between ports of antenna element neutralisation line technique was applied between the antenna structures [Diallo *et al.* (2008a)]. Soon after, Kim *et al.* proposed an innovative design of wideband MIMO antenna with a compact size and low mutual coupling between antennas. The isolation was enhanced mainly because of the orthogonal current paths that oblique placement of two antennas [Kim *et al.* (2008)]. Again, Su *et al.* presented a printed coplanar two-

antenna element suited for WLAN operation in the 2.4- and 5-GHz bands for dual-module applications in a MIMO system. The two-antenna element comprised of one PIFA and one monopole antenna, both printed and integrated in a coplanar configuration on a narrow dielectric substrate with the dimensions of 50 mm × 11 mm. The two antennas were excited using two separate feeds [Su *et al.* (2008)]. In two consecutive months of the year 2008, Chebihi *et al.* and Diallo *et al.* discussed about the neutralization line technique to enhance the isolation between antenna elements and applications of MIMO antenna for UMTS mobile phones. Diversity performance of multi antenna systems for UMTS cellular phones in different propagation environments was also studied [Chebihi *et al.* (2008) and Diallo *et al.* (2008b)]. Later on, Lee *et al.* depicted metamaterial MIMO antenna and each antenna element comprised a top patch, launch pad, via, via pad and via line. The antenna was excited by coupling an L-shape launch pad to the top patch with a gap. The metallic via connected the top patch on one side of the substrate to via pad on the other side of the substrate. Via pad connected to the ground through an L-shape via line [Lee *et al.* (2008)]. Further, Chou *et al.* presented various isolation improvement techniques for MIMO WLAN card bus applications consisted of three closely spaced loop antennas which was verified numerically and experimentally [Chou *et al.* (2008)]. Again, Lui *et al.* described two nearby dual-band antenna structure with high port isolation. The decoupling and matching network was used to improve isolation between ports and network consisted of only reactive elements so that it does not dissipate the input power [Lui *et al.* (2008)].

In 2009, Cai and Gong investigated a novel wideband printed diversity antenna for mobile handsets which consisted of two monopoles with symmetric configuration [Cai and Gong (2009)]. The operational bandwidth was achieved 1860 MHz to 2490 MHz. Later, Bhatti *et al.* proposed a low profile quad band MIMO antenna for portable wireless communications terminals. A combination of a C-shaped slot and a T-shaped slit is used to excite three current modes in a conventional single-band PIFA. A $\lambda/4$ resonator was integrated into the tri-band antenna structure in order to get an additional resonance for quad-band operation

[Bhatti *et al.* (2009b)]. In the same year Wang *et al.* introduced a compact dual-element antenna array for adaptive MIMO system. By four embedded PIN diodes in the feeding network, the antenna array showed three different working states. It could operate as a dual-element antenna array or work as a single antenna while the unselected antenna was terminated to a lumped matched resistor [Wang *et al.* (2009a)]. Further, Choi *et al.* described MIMO antenna systems for mobile WiMAX handset applications [Choi *et al.* (2009)]. In the same year, Zhang *et al.* and Wang *et al.* reported isolation enhancement technique. Zhang *et al.* depicted a two-PIFA antenna system for compact diversity/MIMO terminals which supported PCMCIA card and WLAN. The antenna system exhibited better isolation performance with less inter-antenna spacing between antenna elements [Zhang *et al.* (2009a)]. Wang *et al.* depicted an antenna which composed of a low-profile monopole and a pair of inverted-L antennas fed by 180^0 out-of-phase excitations. The pattern and polarization diversity was achieved by such excitation due to which high isolation was achieved between antenna elements [Wang *et al.* (2009b)]. Soon after, Han and Choi suggested a compact multiband MIMO antenna with a band stop matching circuit for next generation mobile applications which consisted of two dual-band PIFAs that provided wideband characteristics. In order to improve the isolation characteristic at the LTE band, a band stop matching circuit was inserted at the corner of each antenna element [Han and Choi (2009)]. Further, Xiong *et al.* analysed a compact planar MIMO antenna system of four elements with similar radiation characteristics which covered 2.4 GHz WLAN band. It consisted of two proximity-coupled fed microstrip square ring patch antennas and two $\lambda/4$ microstrip slot antennas of the same linear polarization. These two types of antennas were printed on different sides of the substrate to reduce mutual coupling [Xiong *et al.* (2009)]. Further, Li *et al.* demonstrated a dual slot diversity antenna with isolation enhancement using parasitic elements for mobile handsets [Li *et al.* (2009)] while Fakhr *et al.* designed a dual band MIMO antenna, with a compact size and low mutual coupling between antennas. Antennas operated at 2.45 and 5.2 GHz were proposed, which have 10 dB return loss bandwidths of 10.6% and 10.5%,

respectively [Fakhr *et al.* (2009)]. In the same year, Azremi *et al.* (2009) proposed a five-element inverted-F antenna array on mobile terminal for both MIMO communications and Radio Direction Finding (RDF). The multi element antenna (MEA) system was designed to be used in the frequency band of the future LTE system at 3400-3600 MHz and integrated along the edges of the upper ground plane of a clamshell type mobile terminal. Without using any specific multi-antenna isolation techniques, the antennas were optimized to have acceptable mutual coupling and small envelope correlation in order to provide enhanced capacity with MIMO techniques [Azremi *et al.* (2009)]. Later on, Park *et al.* (2009) proposed quad band mobile handset antenna with low correlation. A suspended line between the antenna 1 and antenna 2 was used to improve isolation. Suspended line comprised of meandered transmission line between antennas was able to operate like a band stop filter and lead to the isolation between two ports despite very close distance [Park *et al.* (2009)]. Zhang *et al.* (2009) described a compact printed Ultra Wideband (UWB) MIMO/diversity antenna system (of two elements) with a size of 35 × 40 mm^2 operating at a frequency range of 3.1–10.6 GHz. The wideband isolation could be achieved through a tree-like structure on the ground plane [Zhang *et al.* (2009b)].

In 2010, Rao and Wang suggested a compact integrated dual-port diversity antenna, which was suitable for LTE and Wi-Fi applications in handheld devices. The antenna merged two PIFAs into a single-antenna structure that not only occupied lesser volume in a handheld device but also eliminated the need to separate two individual antenna elements, which provides further space-saving efficiency. This can be accomplished even while maintaining desirable isolation and diversity characteristics [Rao and Wang (2010)]. Later, Tian *et al.* investigated MIMO system which consisted of two three-port DRA elements, which jointly utilizes spatial, polarization and angle diversity. In order to evaluate its performance for WLAN type applications, a 6 × 6 MIMO channel measurement campaign was conducted at 2.65 GHz in indoor scenarios [Tian *et al.* (2010)]. Further, Wei *et al.* (2010) depicted a conformal dual-port diversity patch antenna, operated with a broadside and/or conical radiation pattern,

demonstrated for WLAN applications. The conical and broadside modes were excited separately by using a hybrid feed network [Wei *et al.* (2010)], whereas Yang *et al.* demonstrated a broad dual-band PIFA for the DVB-H service and a dual-band MIMO antenna with high isolation performance for the WLAN service [Yang *et al.* (2010)]. Soon after, Luo *et al.* (2010) described a reconfigurable dual-band monopole array with high isolation for WLAN MIMO application. This antenna array contains two C-shaped monopoles with a shorting line, on which two RF switches were integrated, connected two antenna elements that are separated by a distance of $0.09\lambda_{2.4GHz}$ [Luo *et al.* (2010)]. Later on, Shin and Park designed a magneto dielectric material and its MIMO application for LTE band. The proposed antenna was a folded monopole type and occupied a compact volume of 7.5 × 18.5 × 3.4 mm^3. For reducing the size, obtaining broad bandwidth, and enhancing the isolation performance, the magneto-dielectric material was applied as a supporter [Shin and Park (2010)]. Further, Lee *et al.* proposed a method for isolation improvement of MIMO antennas using a Split Ring Resonator (SRR) array structure between the two radiating elements [Lee *et al.* (2010)]. Kuonanoj investigated low correlated handsets antenna for LTE MIMO application [Kuonanoj (2010)]. Further, Li *et al.* reported a MIMO antenna which consisted of two identical folded monopole antennas each of which has the dimension of 5.1 mm × 10 mm. The separation between the two antennas is 4.8 mm (about 3.8% of the wavelength at 2.4 GHz). In order to realize the good isolation performance for such a small separation, a suspended strip was used to connect the two monopoles together and it forms an effective filter with the ground plane at the required frequency band [Li *et al.* (2010)]. In the same year, Lhilali *et al.* described a multi-band multi-antenna system for WLAN MIMO box with low isolation. The miniaturized antenna consisted of two IFAs antennas placed at the corner of the home-box PCB [Lhilali *et al.* (2010)]. Soon after, Nezhad and Hassani discussed a novel multiband E-shaped printed monopole antenna for MIMO system. The proposed E-shaped monopole antenna was created a single resonance within the WLAN range. Placement of two slots within the E-shaped monopole antenna created two extra resonances whose centre

frequencies were adjusted by the E-shaped monopole and the slots parameters [Nezhad and Hassani (2011)].

In 2011, Han and Choi proposed a compact printed MIMO antenna with an embedded chip inductor for a 4G mobile handset application. The proposed MIMO antenna consisted of a longer strip with an embedded chip inductor and a shorter radiating strip [Han and Choi (2011a)], while Najam *et al.* developed a compact printed and planar MIMO for Ultrawideband communications. Two circular disc monopole antenna elements constituted the proposed UWB-MIMO antenna operated over the frequency band of 3.2−10.6 GHz. The isolation enhancement was achieved by taking the advantage of an inverted Y-shaped stub that was being inserted on the ground plane of UWB-MIMO antenna [Najam *et al.* (2011)]. Later, Kim *et al.* designed MIMO antenna consisted of two PIFAs and two isolators. The PIFAs has a volume of 12×10×4 mm^3, which was small enough to be incorporated in a mobile MIMO terminal. The two isolators were designed symmetrically and placed between the two PIFAs to enhance the isolation performance of the MIMO antenna by suppressing the current flow between the antennas in the 2.3 and 3.4 GHz bands [Kim *et al.* (2011)]. Further, Rao and Wilson presented a new multiband, dual-element diversity antenna system, which was suitable for compact multimode wireless handheld devices. In order to validate the practicality of the proposed system, the antenna was tested in real-world environments, similar to those in which compact wireless handheld devices were expected to operate [Rao and Wilson (2011)]. Later on, Yang *et al.* suggested a method to reduce mutual coupling between extremely closely placed dual-element microstrip antennas. High isolation was achieved through a simple slot structure on the ground between the microstrip antennas [Yang *et al.* (2011)]. Soon after, Cui *et al.* discussed a compact dual-band MIMO antenna with high port isolation. The proposed antenna was basically composed of two folded monopoles and was designed to operate at 2.4/5.6 GHz. The high isolation was achieved by introducing two transmission lines on the top surface of the substrate and etching two slots on the ground [Cui *et al.* (2011)]. Further, Lee *et al.* demonstrated a LTE MIMO ferrite antenna which was fabricated on

$Ni_{0.5}Mn_{0.2}Co_{0.07}Fe_{2.23}O_4$ ferrite substrate ($14 \times 7 \times 3$ mm^3) and characterized for antenna performance. Measured return loss and isolation were -26 dB and -16.4 dB at 720 MHz, respectively [Lee *et al.* (2011)], whereas Wong *et al.* illustrated an antenna array which comprised a main antenna for eight band LTE/WWAN operation and an auxiliary antenna was combined with the main antenna for LTE MIMO operation in the mobile phone. Both the main and auxiliary antennas were disposed at the bottom edge of the system circuit board of the mobile phone and separated by a protruded ground [Wong *et al.* (2011)]. Further, Sharawi *et al.* described a meander line 2-element MIMO antenna system and fabricated for LTE mobile handsets. The antenna system operated in the 700–800 MHz frequency band with a bandwidth of more than 100 MHz [Sharawi *et al.* (2011)]. Later, Ling and Li reported a dual-band MIMO antenna array for portable wireless devices. The MIMO antenna array consisted of two back-to-back monopoles elements with an edge-to-edge distance of 0.096λ (λ is the free-space wavelength at 2.4 GHz). A shorting strip and an isolation stub were designed to reduce the mutual coupling between the two elements [Ling and Li (2011)]. In the same year, Han and Choi discussed a dual-band MIMO antenna and used polarization diversity for a 4G mobile handset application. The proposed MIMO antenna consisted of two printed dual-band PIFAs with a slotted strip. Input port 1 of the first PIFA was orthogonally disposed with respect to input port 2 of the second PIFA. The orthogonal placement of the two feed points ensured the dominant polarization of each of the PIFAs was opposite to each other, resulted in a good isolation performance [Han and Choi (2011b)]. Further, Li *et al.* illustrated a tri-band four-element MIMO antenna with high isolation. Two kinds of isolation structure were applied to enhance the isolation. The first kind of isolation structure consisted of two slits and a protruded ground branch, and the second kind of isolation structure consisted of four symmetrical slits etched on the ground plane [Li *et al.* (2011)]. In the same year, Huitema *et al.* designed a compact multiband antenna which is to be integrated in a tablet, it was not only heavily miniaturized ($\lambda_0/15 \times \lambda_0/38 \times \lambda_0/94$ at 800 MHz), but also able to cover three frequency bands for different wireless applications (DVB-H, WiFi and WiMAX) [Huitema *et al.*

(2011)]. Mansouri and Khaleghi described a compact dual port diversity antenna for LTE (2.5-2.7 GHz) application. The antenna structure was optimized to provide the required bandwidth of 7.7%, isolation of -24 dB, and a small volume [Mansouri and Khaleghi (2011)]. Further, Li and Chu analyzed a proximity-fed MIMO antenna with two printed IFAs and a wideband T-shaped neutralization line. Each element printed IFA was fed by a proximity-fed structure which provided a parameter to control the return loss without any effect on the isolation of the two IFAs [Li and Chu (2011)]. Rafik *et al.* designed a dual band [2.4-2.48 GHz and 5.15-5.725 GHz] multi antenna system with high isolation between the access ports [Rafik *et al.* (2011)]. Further, Li and Chen proposed a novel concurrent 2-port/3-port MIMO antenna system for UMTS/LTE2500 operation in the mobile phone [Li and Chen (2011)]. Later on, Chung *et al.* described a new technique that significantly reduced the antenna correlation. The technique was called as negative group delay technique since it enhanced the isolation between antennas using negative group delay phenomenon [Chung *et al.* (2011)]. Then, Lu *et al.* demonstrated a dual-band 4-port diversity antenna for LTE MIMO applications. The antenna element employed a dual-band design which covered the 700 MHz band for LTE applications and the 2.4 GHz band for WLAN systems [Lu *et al.* (2011)]. Soon after, Tuan described new method of modelling radio communications systems by using MIMO antenna [Tuan (2011)]. Abidin *et al.* revealed a compact dual U-shaped slot PIFA antenna with electromagnetic bandgap material on a relatively low dielectric constant substrate. Periodic structures were found to reduce mutual coupling and decreases the separation of antenna and ground plane [Abidin *et al.*(2011)].

In 2012, Cheon *et al.* delineated a magneto-dielectric material, which was had low magnetic loss and moderate permeability for the wireless communication band [Cheon *et al.* (2012)], while Yan and Bernhard described a novel MIMO dielectric resonator antenna for LTE femtocell base stations. A systematic design method based on perturbation theory was proposed to induce mode degeneration for MIMO operation [Yan and Bernhard (2012)]. In the same month of same year Li *et al.* discussed a method to reduce the mutual coupling by using parasitic

elements. By adding parasitic elements a double-coupling path was introduced and it created a reverse coupling to reduce the mutual coupling [Li *et al.* (2012a)]. Li *et al.* suggested a compact wideband MIMO antenna with two symmetric monopoles and edge-to-edge separation of nearly $0.083\lambda_0$ at 2.5 GHz. Two novel bent slits were etched into the ground plane to reduce the mutual coupling [Li *et al.* (2012b)]. Soon after, Addaci *et al.* proposed a technique to enhance the port isolation. This broadband technique involved in inserting an optimized parasitic element between the two antennas of a MIMO set-top box [Addaci *et al.* (2012)]. Further, Jin *et al.* demonstrated a small-sized (15 mm × 30 mm) planar monopole MIMO antenna that offered high-isolation performance. The antenna was miniaturized using inductive coupling within a meander-line radiator and capacitive coupling between a radiator and an isolator [Jin *et al.* (2012)] while Yu *et al.* presented a compact wideband diversity antenna covering the PCS/UMTS/WiMAX bands with high isolation with low envelope correlation coefficient [Yu *et al.* (2012)]. In the same month of same year, Li *et al.* drawn an extremely compact dual-band MIMO antenna for 4G USB dongle applications for operation in the LTE band 13 (0.746–0.787 GHz) and the M-WiMAX band (2.5–2.69 GHz) [Li *et al.* (2012c)] while Zhang *et al.* revealed an efficient technique to reduce mutual coupling between two closely spaced PIFAs for MIMO mobile terminals. The proposed mutual coupling reduction method was based on a T-shaped slot impedance transformer and could be applied to both single-band and dual-band PIFAs [Zhang *et al.* (2012a)]. Further, Yao *et al.* reported a broadband circularly polarized two-element PIFA with pattern diversity and high isolation for multimode satellite navigation [Yao *et al.* (2012a)]. Again, Chattha *et al.* presented a novel dual-feed PIFA suitable for wireless applications such as WLAN and LTE as a diversity and MIMO antenna. Instead of two antenna elements, there was only one top radiating element with two isolated feeding ports, which saved space and cost [Chattha *et al.* (2012)]. Soon after, Chen *et al.* designed a monopole slot MIMO antenna with compact size for WLAN band (2.4–2.484 GHz) application. By the concept of electromagnetic shield, the antenna module was formed by an open-ended monopole slot surrounded by

another open-ended monopole slot on the ground plane [Chen *et al.* (2012)]. Later on, See *et al.* analyzed a novel printed diversity monopole antenna for WiFi/ WiMAX applications. The antenna comprised two crescent shaped radiators placed symmetrically with respect to a defected ground plane and a neutralization line was connected between them to achieve good impedance matching and low mutual coupling [See *et al.* (2012)]. Foudazi *et al.* proposed a triple band MIMO antenna. By protruded an L-shaped parasitic strip on the ground plane, third band as well as enhancement of the isolation between two ports in MIMO array was achieved [Foudazi *et al.* (2012)]. In the same month Zhou *et al.* developed a dual-broadband MIMO antenna system for GSM1800/ 1900, UMTS2000, LTE2300/ 2600, and WLAN2.4/ 5 GHz communication handsets. The MIMO antenna system was composed of two dual-broadband antenna elements, each of which consisted of an outer loop coupled by an inner loop [Zhou *et al.* (2012)]. Soon after, Lee *et al.* designed a UWB MIMO antenna arrayed on the top part of the wireless device substrate. In addition, parasitic meander lines were located between the arrayed antennas to improve the isolation [Lee *et al.* (2012b)] while Li *et al.* described a compact conventional phone antenna integrated with wideband MIMO antenna. Within operation band of the MIMO antenna, the effect of mutual coupling between the conventional phone antenna and the MIMO antenna was reduced by etching three slits into the ground plane [Li *et al.* (2012d)]. In the same month, Ryu and Woo presented an ultra-wideband MIMO antenna covered WCDMA, WLAN, WiMAX and UWB bands for mobile handset applications [Ryu and Woo (2012)]. Kim *et al.* designed a compact USB dongle MIMO antenna for LTE 700 band applications and constructed it with a modified meander radiator and a capacitively coupled feed line [Kim *et al.* (2012)] while Ssorin *et al.*, presented the three different microstrip MIMO antenna system designed for LTE/WiMAX USB dongle applications operated in the 2.5–2.7 GHz frequency band [Ssorin *et al.* (2012)]. Further, Zhang *et al.* suggested a closely-packed ultra wideband MIMO/Diversity antenna with different patterns and polarizations for USB dongle applications [Zhang *et al.* (2012b)]. Thereafter, Mouffok *et al.* proposed a compact dual-band, dual-polarized antenna for LTE

applications with an extension of the lower band towards TV white space band, to provide radio cognitive capabilities to the terminal [Mouffok *et al.* (2012)]. Soon after, Zhang *et al.* demonstrated a novel dual-band operated MIMO antenna constructed by planar monopole and 3D slot element. A lumped impedance network was introduced in port1, both main antenna and auxiliary antenna matches very well [Zhang *et al.* (2012c)] while Yao *et al.* proposed a novel multiband printed planar monopole antenna for LTE MIMO application consisted of meandering microstrip line loaded on monopole antenna [Yao *et al.* (2012b)]. Further, Meshram *et al.* designed and analysed a novel quad-band diversity antenna with two radiating elements suitable for LTE and Wi-Fi applications in handheld devices. The radiating elements consisted of PIFA constructed by a meandered line and folded patch with interdigitated capacitive strips connected to the folded patch and DGS. DGS helped to improve the isolation between antenna ports and achieved below -24 dB [Meshram *et al.* (2012)]. Ayatollahi *et al.* outlined a compact dual-port, MIMO antenna array for handheld devices whereas two quarter wavelength monopole slots etched on the ground plane of a printed circuit board and a meandered slot cuts between them for high isolation [Ayatollahi *et al.* (2012)]. Soon after, Yang *et al.* proposed two multi patch monopole antennas which were placed 90^0 apart for orthogonal radiation. To strengthen the isolation, a T-shaped ground branch with proper dimension was used to generate an additional coupling path to reduce the mutual coupling [Yang *et al.* (2012)]. Further, Karimian *et al.* presented a new L-shaped slot dipole for MIMO antenna system with an L-shaped slit for WLAN and WiMAX applications [Karimian *et al.* (2012)] while Zheng *et al.* proposed a dual-element small-size printed strip MIMO antenna. A ground plane with a slot and dual-inverted-L-shaped stub was used to decrease the mutual coupling between the antenna elements [Zheng *et al.* (2012)]. Further, Rezaeieh and Pouyanfar described a miniaturized monopole antenna with filtering properties. An *S*-shaped double channel compact MIMO antenna with high isolation performance for DSC1800, PCS1900, WiMAX, and WLAN was presented [Rezaeieh and Pouyanfar (2012)]. In the same month of the same year, Jan *et al.* presented a

novel 4-shaped 2×1 compact dual-band MIMO antenna system that covered the lower LTE band of 858-920 MHz and a higher band from 2955-3130 MHz that was suitable for next generation mobile and handheld wireless terminals [Jan *et al.* (2012)] while Shen *et al.* revealed a antenna which comprised of two back-to-back G-shaped monopoles and placed symmetrically with respect to a T-shaped and dual inverted-L-shaped ground plane [Shen *et al.* (2012)].

In 2013, Zhao *et al.* proposed a compact MIMO antenna with a coupled feed structure for 4^{th} generation handsets for operation in LTE band 13 (0.746 –0.787 GHz) [Zhao *et al.* (2013)] while Fernandez and Sharma demonstrated a low-profile meandered loop antennas with MIMO implementations that covered multiple communication bands for wireless routers and access points [Fernandez and Sharma (2013)]. Further, Wong *et al.* analyzed a highly isolated tri-band WLAN MIMO antenna array for laptop computer applications. A new isolation element formed by a central protruded ground and a spiral open slot embedded therein were shown to effectively enhance the isolation between the antennas [Wong *et al.* (2013)]. Soon after, See *et al.* presented a miniaturised diversity antenna suitable for ultra-wideband. MIMO antenna comprised of two identical PIFAs, a T-shaped structure and a finite ground plane. The T-shaped structure improved the impedance matching and suppressed the mutual coupling between the antenna elements over a wider bandwidth [See *et al.* (2013)] while Zhao and Choi illustrated a wideband loop antennas with distributed elements for fourth generation MIMO mobile terminal. The MIMO antenna system consisted of two wideband loop antenna elements [Zhao and Choi (2013)]. Soon after, Mun *et al.* presented a compact ($5 \times 35 \times 6$ mm^3) handset MIMO antenna constructed with two symmetrical PIFAs for LTE 700 band applications [Mun *et al.* (2013)] while Ojaroudi and Ghadimi described a new design of coplanar waveguide-fed slot MIMO antenna with E-ring radiating stub for WLAN applications [Ojaroudi and Ghadimi (2013)]. Further, Zhang and his group introduced a method to reduce the envelope correlation coefficient with improved total efficiency for mobile LTE MIMO antenna arrays [Zhang *et al.* (2013)]. Abdalla and Ibrahim focused on two element metamaterial MIMO antenna with compact size with high isolation

[Abdalla and Ibrahim (2013)]. Further, Wang and Du used three neutralization lines which was printed on PCB. These lines were used to reduce the mutual coupling within wide frequency band [Wang and Du (2013)].

In the early of 2014, Liao *et al.* designed and studied two closely spaced chip antennas for dual-band wireless LAN applications. A novel isolation enhancement technique was implemented for the higher 5 GHz band, which was done by adding a pair of open-ended stubs next to antenna feeds [Liao *et al.* (2014)]. Cihangir and his group reported two small-size coupling elements with neutralization line operated in the 700-960 MHz frequency band for 4G MIMO operation with good matching, fair efficiency, low envelope correlation coefficient, and high port-to-port isolation [Cihangir *et al.* (2013)], while Wang and Du reported a wideband printed dual-antenna system for mobile terminals which consisted of two symmetric F-like monopoles with two grounded branches which were printed on a PCB [Wang and Du (2014)]. Thereafter, Zhao and his group introduced two L-shaped slots etched on each PIFA appropriately to achieve tri-band and high isolation at higher frequencies [Zhao *et al.* (2014)]. Shoaib *et al.* discussed a novel decoupling structure that consisted of two inverted-L branches and a rectangular slot with one circular end, etched on the ground plane, to achieve low mutual coupling below -15 dB for all matched frequency bands [Shoaib *et al.* (2014)]. Soon after, Lee's research group focused on two PIFAs in conjunction with a T-shaped common radiator. Without using any additional coupling elements between these closely mounted antennas, both high isolation and low envelope correlation coefficient were achieved [Lee *et al.* (2014)]. Further, Ban *et al.* proposed a wide T-shaped protruded ground to enhance the impedance matching and decoupled the two closely deposed antenna elements [Ban *et al.* (2014a)]. Soon after, Dioum *et al.* proposed multiband MIMO antenna consisted of two dual band IFAs. They consisted 3D IFAs folded on the non-metallized part of the PCB [Dioum *et al.* (2014)]. Further, Zhao and Choi proposed a MIMO antenna, designed for 4G mobile systems. By using the resonance of ground planes and the inductive coil, the proposed antenna achieved simplified design, improved bandwidth, and efficiency [Zhao and Choi (2014)]. In

the same year, Al-Hadi *et al.* designed two sets of eight-element antenna structures based on capacitive coupling element and inverted-F antennas operating at 3400–3600 MHz LTE frequency band. The structures were estimated to achieve a good effective diversity gain in both uniform and non-uniform environments [Al-Hadi *et al.* (2014)] while Khan and Sharawi revealed two element multiband MIMO antenna system with miniaturized patch antennas. Antenna miniaturization and multiple band coverage were achieved by the CSRR loading on the individual patch [Khan and Sharawi (2014)]. Later on, Baek and Choi designed a highly isolated MIMO antenna. Decoupling network was proposed which consisted of two sections of a transmission line which was placed at the centre of two radiating elements [Baek and Choi (2014)]. Yang and his group analyzed a dual-band MIMO antenna using the slotted CSRR. The proposed antenna operated in two WLAN bands and possessed high isolation with a slotted CSRR inserted into the ground plane [Yang *et al.* (2014)]. At the end of 2014, Al-Hadi and Tian investigated and generalized multi-element diversity antenna and studied the MIMO performance in small mobile terminal [Al-Hadi and Tian (2014)]. Further, Ban *et al.* proposed a well-decoupled closely spaced heptaband antenna array for WWAN/LTE operation in the smartphone applications. By utilizing the well-designed protruded ground, both isolation and bandwidth were enhanced [Ban *et al.* (2014b)].

In the early 2015, Khan *et al.* illustrated MIMO antenna consisted of two meandered monopole radiators that were decoupled by introducing a folded Y-shaped isolator element between the radiators and isolator [Khan *et al.* (2015)]. Thereafter, Liu *et al.* demonstrated UWB MIMO antenna with two square monopole antenna elements. A T-shaped ground stub and a vertical slot cut on the T-shaped ground stub were used to reduce mutual coupling. Also, two strips on the ground plane were created for notched frequency band [Liu *et al.* (2015)]. Further, Zhao and his group investigated a novel multimode MIMO antenna system composed of a dual element MIMO cellular antenna and dual-element MIMO Wi-Fi antenna for mobile terminal applications. With the multimode excitation, the MIMO cellular antenna was operated at 830–900 MHz, 1700–2200

MHz, and 2400–2700 MHz, for 2G, 3G, and LTE bands, respectively [Zhao *et al.* (2015)]. Soon after, Andujar and Anguera demonstrated MIMO system with investigations of bandwidth, efficiency, correlation, and multiplexing efficiency. MIMO capacity was measured in a reverberation chamber considering a free-space Rayleigh scenario and also included the effect of head and hand phantom [Andujar and Anguera (2015)]. Later on, Shoaib and his group presented a pair of printed coupled fed meandered monopole MIMO antennas for mobile handsets which covered GSM 1800/1900, UMTS, WLAN, and LTE frequency bands [Shoaib *et al.* (2015)].

1.7 Scope of The Thesis

From the foregoing discussion on literature review, it can be said that several papers have been appeared in different peer reviewed journals and conferences but still there is a scope for simplicity, compact structure, high isolation, and compatibility with mobile terminals remains. Therefore, compact MIMO antenna structures with isolation improvement techniques are taken up in this thesis. Consequently, exhaustive simulation and experimental investigations were carried out. The details of which are given in various chapters. The performance evaluation of multiple antennas is taken up in the following Chapter 2.